SOVIET PHYSICS USPEKHI VOLUME 2(68), NUMBER 4 JULY-AUGUST, 1959

IONIZATION IN COLLISIONS BETWEEN IONS AND ATOMS

N. V. FEDORENKO

Usp. Fiz. Nauk 68, 481-511 (July, 1959)

INTRODUCTION

COLLISIONS of ions with gas atoms can result in the detachment or capture of electrons. The cross sections for the ionization and capture processes depend on the relative velocities and structures of the colliding atomic particles.

The basic theory for ionization of atoms by ions in the high-velocity region (energies in the Mev range*) has been given by Bohr.[1] At high velocities the ionization and capture cross sections fall off rapidly with increasing velocity. The shell of the fast particle can retain only those electrons whose orbital velocities are greater than the relative velocity of the colliding particles. According to Bohr, the orbital velocity of the electron in the hydrogen atom is $v_H = e^2/\hbar$ (2.2×10^8 cm/sec). At high velocities ($v \gg v_H$) the ionization of atoms by electrons and heavy atomic particles may be regarded essentially as an impact interaction.

The theory of ionization in atomic collisions in the velocity region $v < v_H$ has not been developed to any great extent. Attempts to extrapolate the concepts used at high velocities to this region have led to disagreement with the experimental observations. Thus, for example, according to Thomson's classical theory of collision ionization[2] the threshold velocity for ionization of hydrogen by heavy particles is

$$v_{min} \cong \frac{1}{2} v_H.$$

This minimum velocity corresponds to energies of several tens or hundreds of kev, depending on the mass of the ion. It is well known, however, that ionization of atoms by ions occurs even in the ev region, as long as the kinetic energy T_0 is greater than the energy threshold T_{min} determined by conservation of energy and momentum:

$$T_{min} = \left(1 + \frac{m_1}{m_2}\right) E_i,$$

where m_1 and m_2 are respectively the masses of the incoming and target particles, and E_i is the first ionization potential of the atom. In the ev region the cross section for ionization increases with increasing T_0.[2,3] At the present time there is good reason to believe that the cross sections for ionization of atoms by ions reach maximum values in the kev region. This range is also of great interest because ion beams in this energy range are used widely in various kinds of machines and instruments, in particular, accelerator injectors, mass spectrometers, etc. The upper layers of the atmosphere are also penetrated by streams of atomic particles in this energy range, which originate in the sun. Ionization at kev energies had not been studied to any great extent until recently, and for this reason little or no information on collisions in gases was published before 1953.[1-7] The first systematic investigations of ionization of hydrogen and helium by ions (energies up to 35 kev) were carried out by Sherwin[8] and Keene.[9] In the course of the last ten years systematic investigations have been in progress at our laboratory on ionization by atomic collision in the energy range between 5 and 180 kev.[10-23] This problem has also been studied by Everhart and his coworkers[24-27] in the U.S.A. (energies from 25 to 150 kev) and by Hasted in England[28] (energies up to 40 kev). In the last few years, ionization has been investigated in gases other than helium and hydrogen. Multiple ionization processes involving the detachment of several electrons have been observed. An analysis of scattering of atomic particles in collisions yields information on the conditions required for various inelastic processes to occur. Firsov[29] and Russek[30] have advanced several new ideas in the theory of atomic collisions to explain recent experimental data. For all these reasons, it seems desirable now to make a rather detailed survey of the problem of ionization in ion-atom collisions.

The present paper has been written with the hope of evaluating and correlating the experimental data obtained in the last few years on ionization of atoms by ions in the kev and ev energy regions. The problem of electron capture has been introduced because in the more complicated cases it is difficult to separate the ionization and capture processes. As is well known, ordinary

*We use the following designation of energy regions: ev, up to 1,000 ev; kev, between 1 and 1,000 kev; Mev, above 1 Mev.

one-electron charge exchange is considered in detail in Chapter 8 of the book by Massey and Burhop.[3]

The first part of the present paper is devoted to a general survey of the data on total ionization cross sections and a comparison of the empirical results with present theoretical predictions. Ionization with detachment of more than one electron is considered in the second part of the paper. In the third part we consider ionizing collisions. Only one kind of atom-ion collision is considered: single collisions of singly charged ions with gas atoms or molecules. This type of collision is of interest in practice and, for this reason, has been widely investigated in recent years. We will call the ion the ionizing particle and the gas atom the target particle. The ionizing particle and the fast atomic particles in different charge states which comprise it will be called the primary ions, and the ions which are formed from the gas atom or gas molecule will be called secondary ions.

I. TOTAL IONIZATION CROSS SECTION

1. Determination of the Total Ionization Cross Section

Collisions of ions (I^+) with atoms (A) can lead to the detachment of electrons from the shells of both colliding particles as a result of the following processes:

$$I^+ + A \rightarrow I + A^{n+} + ne, \tag{1.1}$$

$$I^+ + A \rightarrow I^{k+} + A + (k-1)e, \tag{1.2}$$

$$I^+ + A \rightarrow I^0 + A^{n+} + (n-1)e, \tag{1.3}$$

$$I^+ + A \rightarrow I^- + A^{n+} + (n-2)e, \tag{1.4}$$

where n and k are the charged states of the atomic particles after the collision. We will call the process in (1.1) pure ionization, denoting the cross section by σ^{i}_{0n}, where the lower index 0n indicates the formation of a secondary ion with charge n. The most important process of this kind is one-electron ionization.

The processes in (1.2) involve the detachment of electrons from the shell of the primary ion and are called "stripping" processes. The corresponding cross sections are denoted by σ^{I}_{1k}. It is reasonable to suppose that pure ionization of the atom and stripping of the ion can occur in the same collision.

Processes in (1.3) are called ionization capture processes and the cross sections are denoted by σ^{ic}_{0n}. In these processes secondary ions with charge n are formed, (n − 1) electrons are detached, and one electron is captured in the shell of the primary ion. According to our classification scheme the primary process in this group is ordinary one-electron charge exchange

$$I^+ + A \rightarrow I^0 + A^+.$$

The processes in (1.4) involve the capture of two electrons by the primary ion and the conversion of this ion into a negative ion. The cross sections for these processes are denoted by σ^{icc}_{0n}.

The experimental determination of the total ionization cross section (per unit charge) is usually accomplished by recording the free electrons which appear when an ion beam passes through a gas. This cross section, which is denoted below by σ_-, is sometimes called the global[28] or apparent cross section.[3] Assuming that all the ionization processes listed above can actually occur, we can express σ_- in terms of the appropriate cross sections in the following manner:

$$\sigma_- = \sigma^{i}_{01} + 2\sigma^{i}_{02} + 3\sigma^{i}_{03} + \ldots + \sigma^{I}_{12} + 2\sigma^{I}_{13} + 3\sigma^{I}_{14} + \ldots + \sigma^{ic}_{02} + 2\sigma^{ic}_{03} + 3\sigma^{ic}_{04} + \ldots + \sigma^{icc}_{03} + 2\sigma^{icc}_{04} + 3\sigma^{icc}_{05} + \ldots \tag{1.5}$$

The importance of the individual terms in Eq. (1.5) depends on the relative velocity and the structures of the colliding particles. In the majority of cases the main contribution to the total ionization cross section is that of pure one-electron ionization. In this case

$$\sigma_- \simeq \sigma^{i}_{01}. \tag{1.6}$$

The total ionization cross section is usually measured by the condenser technique.[9,16,28] In making these measurements it is necessary to take care to avoid spurious effects which introduce distortions in the results. In particular, there is danger of electrons produced by secondary emission penetrating into the measurement volume when the ions in the beam strike various electrodes. Hence, longitudinal electric fields which can readily displace the electrons with the ion beam must be avoided. It is also possible to have secondary electron emission from the plates of the measuring condenser itself: these electrons are produced when the plates are struck by secondary ions accelerated by the condenser field. The scattered primary ions which arise in charge-exchange reactions of metastable atoms on the electrode surfaces can also produce secondary electrons. In some recent work,[16,22,23] the condenser plates have been sectionalized to combat masking effects, with the central section being used as the measuring electrode and the outer electrodes as guard electrodes. In front of the plates there are usually shielding grids to constrain the secondary electrons formed on the surfaces of the plates.

TABLE I. Measurements of the total ionization cross section (σ_-) carried out between 1950 and 1958

Pair	Energy range (kev)	Literature reference	Pair	Energy range (kev)	Literature reference	Pair	Energy range (kev)	Literature reference
H^+-H_2	0.4—2.5; 4.6—42.0	28	H^+-Ne	0.9—2.5; 5.2—38.0	28	Na^+-A	10—20	12
»	12.3—36.7	31	H_2^+-Ne	0.4—2.5; 5.0—38.0	28	A^+-A	0.025—2.0; 3.6—39.0	28
»	5—180	21	He^+-Ne	0.1—2.0; 5.0—38.0	28	»	5—25	12
$H_3^+-H_2$	0.4—2.5	28	»	12—177	16	»	12—175	16
»	10—177	21	N^+-Ne	5—30	12	K^+-A	0.15—0.25	33
$H_3^+-H_2$	10—177	21	Ne^+-Ne	0.05—2,0; 5.2—40.0	28	»	0.2—0.9	34
He^+-H_2	0.05—2.5; 5.2—40.0	28	A^+-Ne	0.9—2.5; 5.0—36.0	28	Ba^+-A	5—25	12
Be^+-H_2	5—30	12	»	5—30	12	Pb^+-A	10—20	12
N^+-H_2	2.5—23.0	32	K^+-Ne	0.15—0.25	33	He^+-Kr	3—177	16
Ne^+-H_2	0.4—2.5; 5.2—29.0	28	»	0.20—0.90	34	N^+-Kr	5—30	12
A^+-H_2	0.1—2,4; 5.2—34.0	28	Pb^+-Ne	10—20	12	A^+-Kr	0.025—2.3; 5.2—40.0	28
»	2.4—23.0	32	H^+-A	0.4—2.5; 5.2—40.0	28	»	5—30	12
Kr^+-H_2	5—25	32	»	5—180	22	»	12—173	16
H^+-He	0.4—2.5; 5.2—40.0	28	H_2^+-A	0.1—2,4; 5.2—38.0	28	K^+-Kr	0.075—0.250	33
H_2^+-He	0.4—2.5; 7.0—40.0	28	»	5—177	22	»	0.2—0.6	34
He^+-He	0.05—3.3; 8.4—42.0	28	H_3^+-A	15—177	22	Kr^+-Kr	0.15—2.4; 5.2—18.0	28
»	5—30	12	He^+-A	0.025—3.6; 5.2—38.0	28	Ba^+-Kr	10—20	12
»	12—175	16	»	5—30	12	K^+-Xe	0.1—0.25	33
Be^+-He	10—30	12	»	3—175	16	A^+-N_2	0.1—3.6; 3.6—36	28
N^+-He	5—30	12	Be^+-A	5—30	12	Ba^+-N_2	5—30	12
Ne^+-He	0.4—2,4; 5.2—38.0	28	N^+-A	5—30	12	H^+- air	5—180	23
A_2^+-He	0.4—2,4; 5.2—38.0	28	Ne^+-A	0.05—2.5; 4.5—40.0	28	H_2^+- air	5—180	23
»	5—30	12	»	5—30	12			
			»	10—178	16			

The measurement condenser is usually located in a so-called collision chamber where, by means of narrow slits and differential pumping, it is possible to maintain the gas pressure somewhat higher than in the other parts of the system. To produce conditions favorable for single ionizing collisions, the pressure in the collision chamber must be kept low (1 to 3×10^{-4} mm Hg).

The condenser technique can also be used in making estimates of the energies of the electrons that are detached in ionization. According to the data of references 8 and 9, the majority of electrons have energies not more than a few electron volts.

2. Experimental Data on the Total Ionization Cross Section

A rather comprehensive review of the work carried out up to 1950 on total cross sections for ionization of atoms by ions is given by Massey and Burhop.[3] It should be noted that the early data, particularly in the ev region, are highly inconsistent. The results of the more recent work, however, are more consistent. A list of the ion-atom pairs which have been investigated between 1950 and 1958 is given in Table I.

The available data on total ionization cross sections refer mainly to four inert gases — helium, neon, argon and krypton — and two molecular gases — hydrogen and nitrogen. The greatest number of measurements has been made with argon and hydrogen. The ionizing particles used mostly are He^+, Ne^+, A^+, Kr^+, the hydrogen ions H^+, H_2^+, H_3^+, and ions of the alkali metals. The data for ions of the alkali metals apply primarily to the ev energy range.

The experimental data accumulated at the present time for various ion-atom pairs lead to certain empirical conclusions as to the influence of such factors as atomic structure and relative velocities on the total ionization cross sections.

The effect of atomic structure can be ascertained by studying ionization of different gases by the same ion. In Fig. 1 is shown the energy dependence of σ_- for He^+ ions in four inert gases

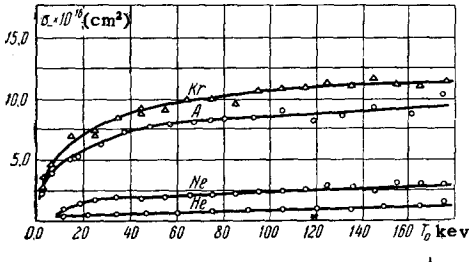

FIG. 1. Total ionization cross section for He^+ ions in helium, neon, argon, and krypton as a function of ion energy. [Data of Fedorenko, Afrosimov and Kaminker.[16]]

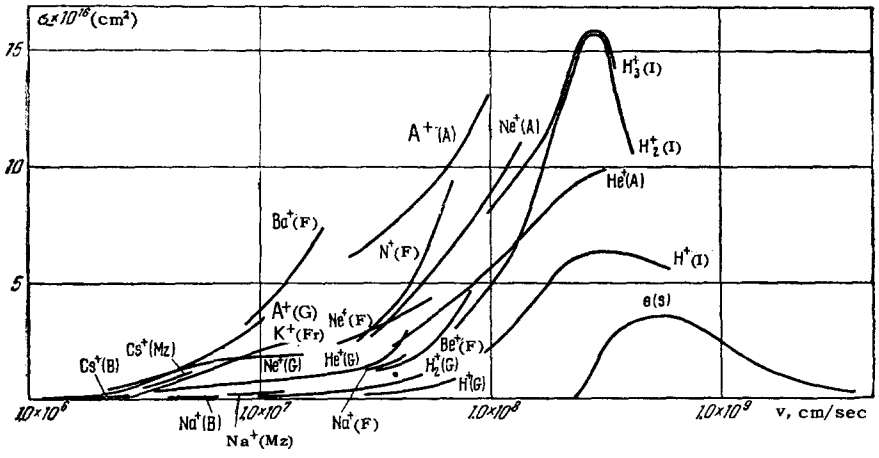

FIG. 2. Total ionization cross section for ionization of argon by various ions as a function of velocity. [G) Gilbody and Hasted;[28] I) Afrosimov, Il'in and Fedorenko;[22] A) Fedorenko, Afrosimov and Kaminker;[16] F) Fedorenko;[12] Mz) Mouzon;[36] B) Beek and Mouzon;[35] Fr) Frische;[37] S) Smith;[38] (ionization by electron impact)].

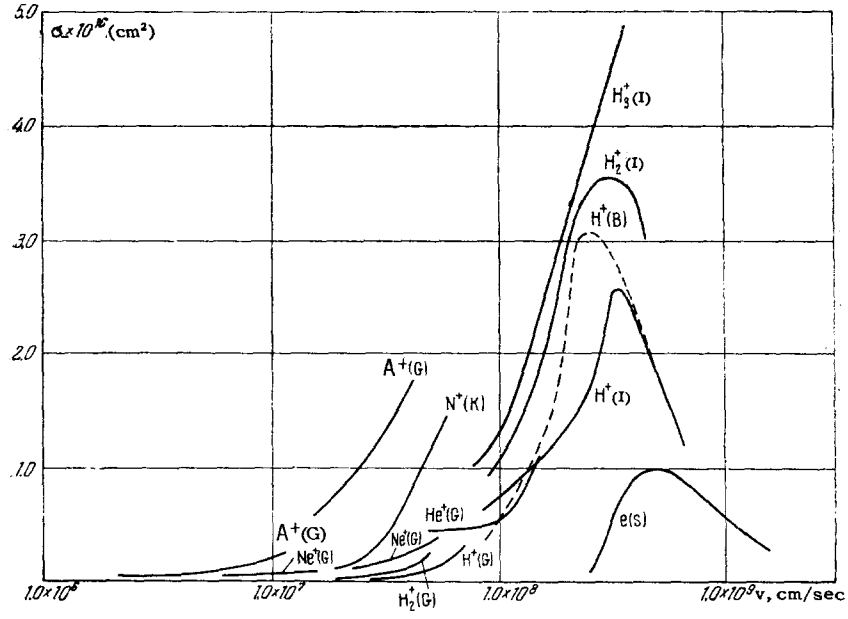

FIG. 3. Total ionization cross section for hydrogen by various ions as a function of velocity. [G) Gilbody and Hasted;[28] I) Afrosimov, Il'in and Fedorenko;[21] K) DeHeer, Huizenga and Kistemaker;[32] B) Bates and Griffing[40] (theoretical curve); S) Tate and Smith[39] (ionization by electron impact).]

as reported in reference 16. It is apparent that for a given ion energy the cross section increases with increasing atomic number of the target atom. The curves in Fig. 1 also give us some idea of the energy dependence of σ_- in the kev energy range. As the energy increases, there is initially a rapid increase in cross section, and then the curve reaches a flat maximum. For the Ne^+-Kr pair and $T_0 = 60$ kev, σ_- increases to approximately 1×10^{-15} cm^2.

The effect of primary ion structure on the velocity dependence of σ_- can be ascertained by an analysis of the data on ionization of argon and hydrogen by different ions, given in Figs. 2 and 3 respectively. To facilitate a comparison of ions of greatly unequal mass the total cross section is given as a function of the logarithm of the velocity of the ionizing particle. The velocity range $10^6 - 10^7$ cm/sec corresponds to an energy range of 0.1 to several kev for ions of unequal mass while the range $10^7 - 10^8$ cm/sec corresponds to several times ten kev for light ions (H^+, H_2^+, and H_3^+) and several hundred kev for heavy ions.* For purposes of comparison, we have also given curves for ionization by electron collision at $10^8 - 10^{10}$ cm/sec, published by Smith.[38] The $\sigma_-(v)$ curves are taken from recent work[12,22,28] and some well-known earlier work.[35,36,37] The ion-atom pairs have been chosen in such a way as to include data for a wide velocity range. An examination of the curves in Figs. 2 and 3 obtained by different authors in different velocity ranges for the same ion (H^+, H_2^+, He^+, Ne^+, A^+) incicates that the agreement over a wide velocity range is fairly good.

According to references 21, 22 and 23 σ_- passes through a maximum only for H^+, H_2^+ and

*The ion energy can be found from the $\sigma_-(v)$ curves in Figs. 2 and 3 through the relation $T_0 = 2.28 \times 10^{-13} v^2 A$ kev, where v is the velocity of the ion in cm/sec and A is its mass in atomic units.

TABLE II. Data on the maximum values of the total ionization cross section

Pair	σ_{-max} (cm²)	T_{0max} (kev)	v_{max} (cm/sec)	v_{max}/v_H	Literature reference
H^+—A	6.7×10^{-16}	~60	3.4×10^8	~1.5	22
H_2^+—A	16.0×10^{-16}	~90	2.9×10^8	~1.3	22
H_3^+—A	16.2×10^{-16}	~105	2.6×10^8	~1.2	22
e—A	3.7×10^{-16}	0.09	5.6×10^8	~2.6	38
H^+—H_2	2.6×10^{-16}	~55	3.2×10^8	~1.5	21
H_2^+—H_2	3.8×10^{-16}	~105	3.2×10^8	~1.5	21
e—H_2	1.0×10^{-16}	0.07	4.9×10^8	~2.3	39
H^+—air	6.3×10^{-16}	~60	3.4×10^8	~1.5	23
H_2^+—air	12.0×10^{-16}	~140	3.6×10^8	~1.7	23

H_3^+ in hydrogen, and for H^+ and H_2^+ in argon and in air. The cross section, velocity, and ion energy for these cases are shown in Table II. The ratio v_{max}/v_H is given in Column 5 of Table II; for comparison we also show the corresponding data for ionization by electron impact.[38,39] The maxima on the $\sigma_-(v)$ curves for hydrogen ions occur at $v \sim 1.5\ v_H$. Most of the available $\sigma_-(v)$ curves for the heavier ions pertain to the velocity region $v < 1.5\ v_H$. All these curves are increasing functions. If it is assumed that for the heavier ions the $\sigma_-(v)$ curve passes through a maximum when $v \sim 1.5\ v_H$, then the energy corresponding to the maximum varies from several hundred kev to several Mev, depending on the ion.

The available data allow us to discuss the effect of the primary ion structure only in terms of a comparison for different ions in the same gas (argon or hydrogen) in the region before the $\sigma_-(v)$ curve reaches its maximum. Comparing the data for atomic ions, we note the following general features: for a given velocity the cross section increases with increasing charge of the nucleus of the primary ion. However, in Figs. 2 and 3 there are a number of exceptions to this general rule. Hasted[28] has proposed a somewhat different relation. This author notes that the "symmetric pairs," i.e., Ne^+-Ne, A^+-A, etc., are especially efficient with respect to ionization. However, it is apparent from Fig. 2, for example, that σ_- for Ba^+-A is larger than for A^+-A. Furthermore, it should be noted that in the heavy ions the contribution of stripping to σ_- is always greater.[12]

The effect of the molecular structure of the primary ion can be understood from a comparison of the cross sections for hydrogen ions themselves. From Figs. 2 and 3 it is apparent that the ionization cross sections for the molecular hydrogen ions H_2^+ and H_3^+ are considerably higher than for protons. In ionization of molecular hydrogen the maximum value of σ_- is approximately proportional to the number of protons contained by the primary ion.

3. Interpretation of the Data on Total Ionization Cross Sections

In the two simplest cases, namely the pairs H^+-H and H^+-He, the ionization cross sections for hydrogen and helium atoms in the kev energy region have been computed by Bates and his colleagues[40,41] in the Born approximation. Using the data for H^+-H Bates and Griffing have obtained a $\sigma_-(v)$ curve for the pair H^+-H_2; this curve is shown in Fig. 3. The maximum on the theoretical curve corresponds to a lower value of the velocity than the maximum on the experimental curve given in reference 21. For $v \geqq 1.5\ v_H$ the theoretical and experimental data are in satisfactory agreement. Below for $v < 1.5\ v_H$ the theoretical values of the ionization cross section are higher. This discrepancy is not surprising since the extrapolation of the Born approximation results to the velocity region $v < v_H$ is open to question.

In interpreting ionization data it is tempting to use the approach used successfully in the interpretation of one-electron charge exchange, i.e., the quasi-adiabatic analysis suggested by Massey.[3] According to this analysis, in an elastic process in which the internal energy changes by an amount ΔE (resonance defect), the cross section reaches a maximum when

$$\frac{|\Delta E|\,a}{\hbar v} \simeq 1, \qquad (3.1)$$

where v is the velocity of the primary particle and a is a quantity of the order of the gas-kinetic diameter, which characterizes the dimensions of the interaction region. The experimental investigations carried out by Hasted[42-45] indicate that in one-electron charge exchange the quasi-adiabatic hypothesis explains the increase in velocity corre-

sponding to the position of the maximum as the resonance defect increases. However, it is still impossible to make a systematic survey of the data on ionization in order to verify (3.1), because the data on the maxima of the $\sigma_-(v)$ curve are still inadequate.[46]

Another result of the quasi-adiabatic hypothesis is that the cross section for inelastic processes must be very small compared with the gas-kinetic cross section when

$$\frac{|\Delta E|a}{\hbar v} \gg 1. \qquad (3.2)$$

As has been noted by Hasted,[28] ionization apparently includes a number of inelastic processes in which (3.2) is not satisfied. One is also convinced of this fact from the data in Fig. 2 for ionization of argon by Ne^+, K^+, A^+ and Ba^+. Hence, the ionization data cannot be interpreted exclusively in terms of the quasi-adiabatic hypothesis.

It was suggested a long time ago[47,48] that there might be a "strong interaction" in atomic collisions at low energies. This suggestion implies that an ionization collision involves penetration of the shell and the excitation of many electrons. The resulting system can be regarded as an excited quasi-molecule with a lifetime τ of $10^{-15} - 10^{-14}$ sec., i.e., a lifetime considerably larger than the oscillation period of the outer electrons in the atom (10^{-16} sec). It is assumed that the excitation energy of the quasi-molecule is dissipated in auto-ionization rather than radiation. This assumption is based on the fact that the lifetime of the excited state for a radiative transition ($10^{-10} - 10^{-8}$ sec) is much larger than τ while the lifetime with respect to auto-ionization is of the same order as τ. The quantum-mechanical analysis of a quasi-molecule, which is required in order to determine the ionization cross section, is a problem of great mathematical difficulty.

Recently, Russek[30] has advanced a new suggestion concerning ion-atom collisions in which ionization occurs; this approach is similar to the quasi-molecule hypothesis, but semi-classical ideas are used in the mathematical analysis. According to Russek the ionization mechanism is analogous to the evaporation of molecules from the surface of a heated liquid. The collision is regarded as a two-stage process. In the first stage, part of the kinetic energy of the relative motion of the particles is converted into excitation energy by virtue of a kind of "friction." In the second stage this energy, which is analogous to thermal energy, is distributed among the electrons, causing partial "evaporation" of electrons. The probability of forming different charge states in the colliding atomic particles is computed as a function of the collision parameters. The Russek analysis has been applied in the interpretation of scattering of ions in which several electrons are removed. The choice of several of the basic parameters in the analysis was made on a rather arbitrary basis in order to obtain best agreement with the experimental data reported by Everhart.[26] Hence, the Russek analysis, as is indicated by its author, is essentially a phenomenological one.

Another attempt at a mathematical development of the quasi-molecule hypothesis by semi-classical methods has been made recently by Firsov.[29] The Firsov theory, in contrast with the Russek theory, allows us to carry out calculations of the ionization cross sections without introducing arbitrary parameters. Firsov starts from the assumption that the spacing between the levels of the quasi-molecule are small compared with the total excitation energy and that the adiabaticity condition is violated even at small velocities. The conversion of the kinetic energy of the relative motion of the colliding particles into excitation energy is regarded as the result of the transfer of momentum by electrons from one particle to the other in the region in which the shells overlap. The magnitude of the excitation energy depends on the collision parameters and determines the ionization probability. Firsov has computed the ionization cross section as a function of the relative velocity and nuclear charges of the ion (Z_1) and the atom (Z_2). The ionization cross section is expressed in terms of an approximate universal formula:

$$\sigma = \sigma_z[(v/v_z)^{1/5} - 1]^2. \qquad (3.3)$$

In Eq. (3.3) σ_Z and v_Z are respectively the characteristic cross section and the velocity for each pair of colliding particles:

$$\sigma_z = \frac{32.7}{(Z_1 + Z_2)^{2/3}} \cdot 10^{-16}\ \text{cm}^2, \qquad (3.4)$$

$$v_z = \frac{25.3E_i}{(Z_1 + Z_2)^{2/3}} \cdot 10^6\ \text{cm/sec}. \qquad (3.5)$$

In Eq. (3.5) E_i is the first ionization potential of the gas atom (in ev). In this case Eq. (3.3) should give the sum of the cross sections for all ionization processes (with removal of electrons from the shells of both particles) for which the required energy is equal to or greater than the energy required for one-electron ionization of the gas atom. The total ionization cross section σ_- does not correspond strictly to the cross section determined from the Firsov formula because in the expression for σ_- [cf. Eq. (1.5)] the cross sections for the elementary processes enter with coefficients which

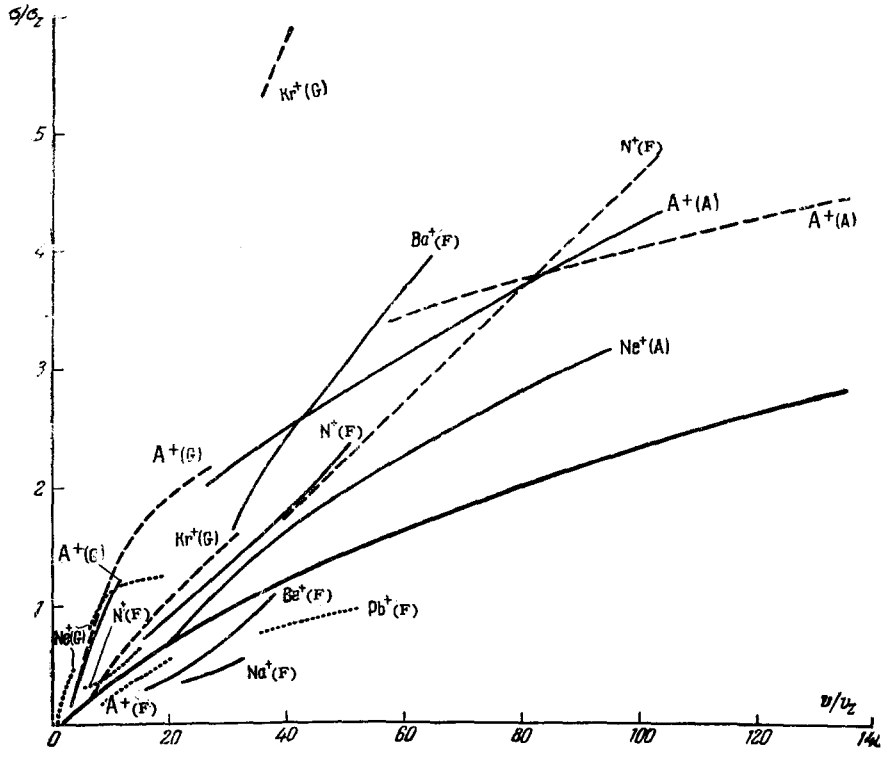

FIG. 4. Universal velocity dependence of the total ionization cross section as given by Firsov[29] (thick solid curve). The experimental data are as follows: G) reference 28, F) reference 12, A) reference 16. The experimental curves for ionization of argon are given by the continuous curves, for krypton by the dashed curves. The designations of the primary ions are given in the figure. The dotted curves refer to ionization of neon.

are equal to the number of detached electrons.

Figure 4 shows a theoretical curve obtained by Firsov and the experimental curves for the total ionization cross section in neon, argon, and krypton by different ions, normalized in accordance with Eqs. (3.4) and (3.5). The experimental data for σ_- are taken from references 12, 16 and 28. Data are given only for ions whose shells contain at least five electrons. This supplementary condition, which is introduced in order to justify the application of statistical ideas, is satisfied by 12 ion-atom pairs which have been investigated in the work cited. It is apparent from Fig. 4 that when v/v_Z changes from 20 to 1.40 the experimental and theoretical data are in agreement to within approximately a factor of 2. The indicated variation of v/v_Z corresponds to a velocity range of 7×10^6 to 9×10^7 cm/sec for different ions. The single exception is the pair $Kr^+ - Kr$, for which the value of σ_- measured in reference 28 is very large (at 40 kev $\sigma_- \sim 1.7 \times 10^{-15}$ cm^2). This particular case requires additional verification because σ_- undergoes a strange discontinuity in the interval between the two velocity ranges for which the measurements have been carried out in reference 28.

It is interesting to note that the experimental $\sigma_-(v)$ curves for $H^+ - A$ and $He^+ - A$ from references 16 and 22 [normalized in accordance with Eqs. (3.4) and (3.5)] are also in agreement with the Firsov theory within the limits of a factor of two (these are not shown in Fig. 4). The only difference is that these curves lie below the Firsov curve while the curves for the other ions are generally above the Firsov curve. Thus, in the velocity range $1 \times 10^7 - 1 \times 10^8$ cm/sec, the Firsov theory gives the correct order of magnitude for the total ionization cross section and describes its variation as a function of velocity. At higher velocities the statistical ideas may not apply and hence one does not expect agreement between theory and experiment. For $(v/v_Z) < 20$, i.e., in the low-velocity region, the discrepancy between theory and experiment is greater than a factor of two. The origin of this discrepancy is not known.

It is more than likely that the total ionization cross section depends on other parameters beside the velocity and charges of the colliding particles. It is reasonable to assume that the cross section is affected by the features of the level systems in the ion and atom.

In order to reveal departures from the universal dependence proposed by Firsov, and to verify the theory further, it will be necessary to acquire a great deal of data for different ion-atom pairs and to make more accurate measurements. The accuracy in the measurement of σ_- is usually estimated by experimenters as 10 — 15%. However, in point of fact the data of various authors are almost always divergent by something of the order of a factor of two. It appears likely that the origin of these discrepancies lies in the sys-

tematic errors which have not been taken into account.

II. IONIZATION WITH THE FORMATION OF MULTIPLY CHARGED IONS

4. Experimental Determination of the Cross Sections

In collisions in the Mev energy region, the atomic shells are highly distorted and multiply-charged ions are formed. In the last few years this effect has been studied by the Soviet physicists Nikolaev and Teplova, and others.[49,50]

It has been established that multiply-charged ions are also formed in the kev energy region. In investigations of multiply charged ions great value attaches to the careful control of collision "multiplicity." The "equilibrium-charge" method[53] is not very convenient for these measurements. A single inelastic collision of atoms or molecules may be accompanied by several elementary processes which result in the detachment or capture of electrons, dissociation, and optical excitation. The exact description of inelastic collisions must contain the quantum state of the particles emitted in the interaction and the particles which are products of the collision. Existing experimental methods do not allow us to determine the cross sections for the elementary processes as defined by these requirements. These methods consist essentially of a measurement of the cross section for the formation of primary or secondary particles in definite charge states. The charge state of the other atomic particle which takes part in the collision generally remains unclear.

For example, secondary ions with a charge n may appear in a gas as a result of pure ionization of the gas atoms or as a result of ionization with capture of one or two electrons in the shell of the primary ion (cf. Sec. 1). The corresponding cross section for the formation of the secondary ions is expressed as follows:

$$\sigma_{0n} = \sigma^{i}_{0n} + \sigma^{ic}_{0n} + \sigma^{icc}_{0n}. \qquad (4.1)$$

Fast neutral atoms may, for example, appear in the primary beam as a result of ordinary one-electron charge exchange or as a result of processes involving ionization with the capture of one electron and the formation of secondary ions with various charge states. The corresponding cross section for the formation of fast atoms σ_{10} is expressed as follows:

$$\sigma_{10} = \sigma^{ic}_{01} + \sigma^{ic}_{02} + \sigma^{ic}_{03} + \ldots \qquad (4.2)$$

The cross sections for the transformation of primary particles are usually determined by a mass-spectrometer analysis of the primary beam after it has passed through the gas. In experiments of this kind it is extremely important to take account of the scattering that accompanies the inelastic processes. The output aperture of the collision chamber must be much larger than the input aperture. The most appropriate object of study is the angular distribution of particles of a given charge; this distribution is then integrated to find the total cross section.[14]

The cross sections for the formation of secondary ions can also be determined by mass spectrometer methods. In the majority of cases these ions have small initial velocities. Hence they are usually extracted from the collision chamber by an electric field and then are accelerated before reaching the analyzer. This method was used by Keene[9] and Lindholm[51,52] to determine the ratios of the various secondary ion cross sections. The use of this method in conjunction with the condenser technique in our work has made it possible to measure the absolute values of cross sections.[17,21-23] Investigation of the energy distribution of the secondary ions (cf. below) has shown that this quantity depends on the charge of the ion and the mass ratio of the colliding particles. Thus, in many cases the estimates of the cross sections for the formation of secondary ions with high charge are too low.[19]

5. Formation of Secondary Atomic Ions

A summary of the available data on the formation of secondary atomic ions (including fragments) in the kev energy region is given in Table III. In some cases the cross sections have not

TABLE III. Data on the secondary ions observed in ionization of atoms and gas molecules by singly charged ions in the kev energy region.

Pair	Secondary ions	Literature reference
H^+—He	(He^+)	9
H_2^+—He	(He^+)	9
He^+—He	He^+, He^{2+}	17
He^+—Ne	Ne^+, Ne^{2+}, Ne^{3+}	17
A^+—Ne	(Ne^+), (Ne^{2+}), (Ne^{3+})	18
H^+—A	A^+, A^{2+}, A^{3+}, A^{4+}	22
H_2^+—A	A^+, A^{2+}, A^{3+}, A^{4+}	22
H_3^+—A	A^+, A^{2+}, A^{3+}, A^{4+}	22
He^+—A	A^+, A^{2+}, A^{3+}, A^{4+}, A^{5+}	17
Ne^+—A	A^+, A^{2+}, A^{3+}, A^{4+}, A^{5+}	17
A^+—A	A^+, A^{2+}, (A^{3+}), (A^{4+}), (A^{5+}), (A^{6+})	17,18
He^+—Kr	Kr^+, Kr^{2+}, Kr^{3+}, Kr^{4+}, Kr^{5+}	17
A^+—Kr	Kr^+, Kr^{2+}, Kr^{3+}, Kr^{4+}	17
H^+—H_2	H_2^+, H^+	21
H_2^+—H_2	H_2^+, H^+	21
H_3^+—H_2	H_2^+, H^+	21
He^+—H_2	(H_2^+)	9
H^+—N_2	N_2^+, N^+, N^{2+}	23
H_2^+—N_2	N_2^+, N^+, N^{2+}	23
H^+—O_2	O_2^+, O^+, O^{2+}, (O^-)	23
H_2^+—O_2	O_2^+, O^+, O^{2+}, (O^-)	23

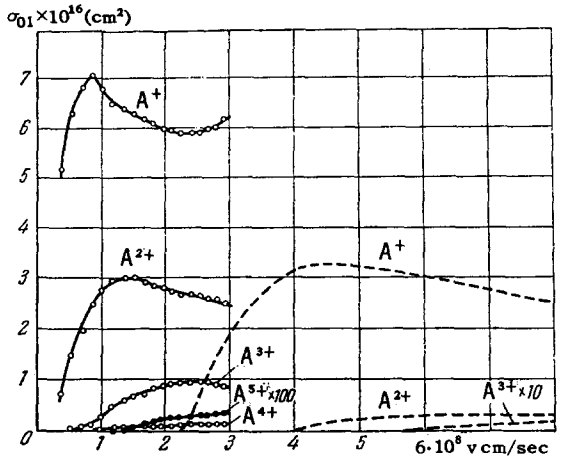

FIG. 5. Formation of secondary argon ions with charge 1, 2, 3, 4 and 5 in ionization of argon by He^+ ions according to Fedorenko and Afrosimov[17] (solid curves) and argon ions with charge 1, 2, 3 in electron impact according to Bleakney[54] (dashed curves). The cross section in units of 10^{-16} cm^2 is plotted along the vertical axis and the velocity of the ionizing particles in cm/sec is plotted along the horizontal axis.

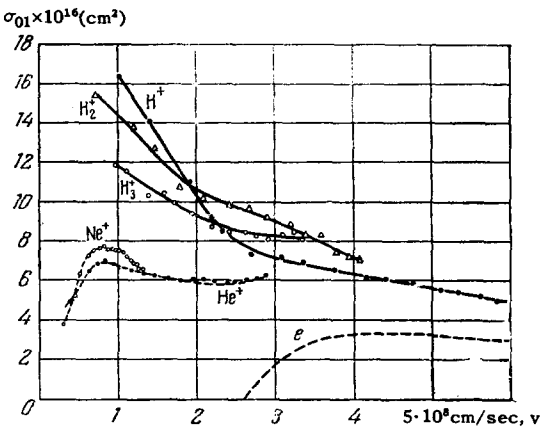

FIG. 6. The cross section for the formation of singly-charged secondary argon ions as a function of the velocity of the primary H^+, H_2^+, H_3^+, He^+ and Ne^+ ions (data of Afrosimov, Il'in and Fedorenko[17,22]) and electrons (data of Bleakney[54]). The designations of the primary ions are given in the figure.

been measured or only lower limits are known: these ions are given in parentheses.

The cross sections for the formation of ions with different charge in electron-atom collisions have been measured by Bleakney.[54] A comparison of the data on analogous cross sections for the formation of secondary ions using the same velocity for ions and electrons indicates a qualitative difference. Figure 5 shows $\sigma_{0n}(v)$ in argon for ionization by He^+ ions and electrons. The formation of argon ions with charge ranging from 2 to 5 in ionization by He^+ ions is observed in velocity regions which are far below the velocity threshold for ionization by electron impact (approximately 2.4×10^8 cm/sec). Furthermore, the maximum cross sections for the formation of doubly-charged ions are approximately ten times (for triply-charged ions, approximately one hundred times) greater than for electron impact. In general the cross sections σ_{04} and σ_{05} could not be measured reliably by Bleakney.

The features noted are in qualitative agreement with the picture of a strong interaction in atomic collisions in the velocity region $v < v_H$.

According to the classical theory of impact ionization given by Thomson[2] the threshold and maximum for ionization in ion-atom collisions should be lower than for electron impact. However, the differences observed in the experiments are much greater than those predicted by this theory.

According to Eq. (4.1), each $\sigma_{0n}(v)$ curve for the formation of secondary ions with charge n represents the superposition of the curves: $\sigma_{0n}^{i}(v)$ and $\sigma_{0n}^{ic}(v)$ (since the contribution due to ionization with two-electron capture is relatively small[55,56]). For example, σ_{01} is the sum of the cross sections for one-electron charge exchange σ_{01}^{ic} and one-electron ionization σ_{01}^{i}. In this case the maximum in $\sigma_{01}(v)$ is apparently related to the maximum in the cross section for one-electron charge exchange. This interpretation is verified by the data of reference 16, in which the total capture cross section was measured. The maxima for $\sigma_{02}(v)$ and $\sigma_{03}(v)$ in Fig. 5 lie in the velocity range $v < v_H$, and in analogy with the preceding case, may be attributed to maxima in $\sigma_{02}^{ic}(v)$ and $\sigma_{03}^{ic}(v)$. The maxima in the curves for pure ionization $\sigma_{02}^{i}(v)$ and $\sigma_{03}^{i}(v)$ probably occur at higher velocities, as is the case for stripping processes (cf. below, Sec. 7).

Certain conclusions as to the effect of the structure of the primary ions on the cross sections can be obtained from an analysis of the curves in Figs. 6 and 7; these curves show the functions $\sigma_{01}(v)$ and $\sigma_{03}(v)$ for ionization of argon by H^+, H_2^+, H_3^+, He^+ and Ne^+ from the data of references 17 and 22. It is apparent from Fig. 7 that for a given velocity σ_{03} increases with increasing charge of the primary ion if it is atomic (H^+, He^+, Ne^+), or with increasing atomic number if it is molecular. The same behavior, but not as well defined, is observed in the total ionization cross section (Sec. 2). This behavior seems to be a feature of all processes characterized by relatively high energy requirements.

On the other hand, this behavior is not observed for σ_{01} (cf. Fig. 6). Apparently this is due to the fact that the basic contribution to σ_{01} is due to one-electron charge exchange, which is a sensitive function of the structure of the outer levels.

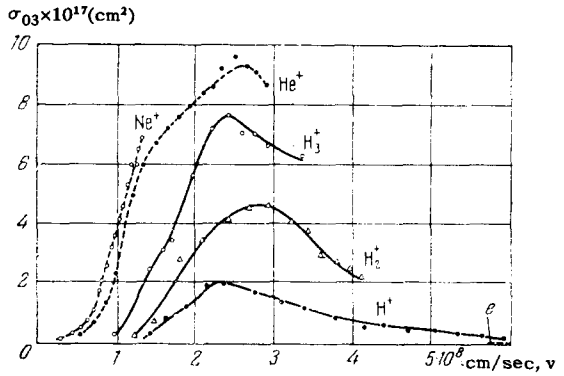

FIG. 7. The cross section for the formation of triply-charged secondary ions of argon as a function of the velocity of the primary H^+, H_2^+, H_3^+, He^+ and Ne^+ ions (data of Afrosimov, Il'in and Fedorenko[17,22]) and electrons (data of Bleakney[54]). The designations of the primary particles he are indicated on the curves.

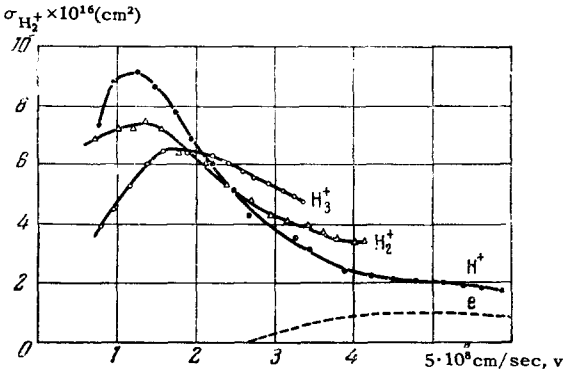

FIG. 8. The cross section for the formation of secondary H_2^+ ions in molecular hydrogen as a function of the velocity of the primary H^+, H_2^+ and H_3^+ ions (data of Il'in, Afrosimov and Fedorenko[21]) and electrons (data of Newhall[57]). The designations of the primary particles are given in the figure.

6. Formation of Fragment Secondary Ions

The secondary ions that are formed as a result of dissociation of gas molecules in ion-molecule collisions are called fragment ions. The dissociation of molecules by electrons and fast atomic particles takes place as a result of a molecular transition to an unstable electronic state and the operation of the Franck-Condon principle. For a secondary ion to be formed, this state must be an ionized state. The removal of electrons from the molecular shell in electron impact is possible only by pure ionization. In ion-molecule collisions dissociation can also take place as a result of capture of electrons from the shell of the molecule by the primary ion.

Electron capture in the dissociation of molecules with the formation of fragment ions has been studied by Lindholm.[51,52] Lindholm has shown that the probability for the formation of fragment secondary ions as a result of dissociation capture, like the probability for usual one-electron charge exchange in ions and atoms, depends on the magnitude of the resonance defect [cf. Eq. (3.1)]. The magnitude of the resonance defect in the present case must be taken as the difference in the recombination energy of the primary ion and the so-called "vertical energy" of dissociation. The vertical dissociation energy is the energy required for a Franck-Condon transition from the ground electronic state to the excited state in which dissociation is possible.[3] In the experiments carried out by Lindholm the primary ion energy was of the order of 500 ev. Lindholm assumes that in the ev region the dissociation energy is a function of electron capture only.

On the other hand, in a theoretical paper by Salpeter[67] it has been shown that in the Mev energy region dissociation in collisions between molecular ions and atoms depends chiefly on the electron detachment. Apparently these and other processes can occur in the kev energy region.

Afrosimov et al.[21] measured the cross sections for the formation of the secondary ions H_2^+ and H^+ in the passage of hydrogen ions H^+, H_2^+ and H_3^+ with energies ranging from 5 to 180 kev through molecular hydrogen. Figures 8 and 9 show the cross sections $\sigma_{H_2^+}$ and σ_{H^+} as functions of the velocity of the primary ions and the analogous cross sections for electron impact according to the data of reference 57. It is apparent that $\sigma_{H_2^+}(v)$ and $\sigma_{H^+}(v)$ have maxima below the thresholds for the formation of the same ions in electron impact. According to the data of reference 57, the cross section for the formation of fragment protons reaches a maximum of approximately 4×10^{-19} cm^2; in ionization of molecular

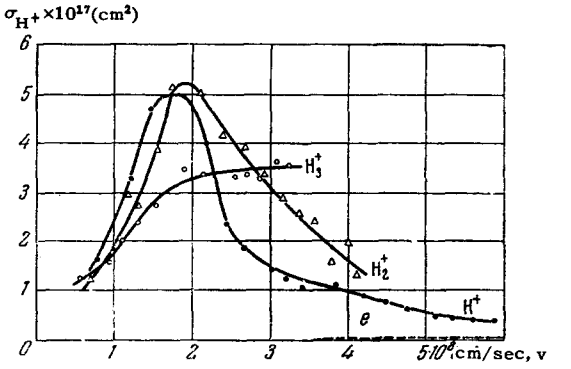

FIG. 9. The cross section for the formation of secondary fragment protons in molecular hydrogen as a function of the velocity of the primary H^+, H_2^+ and H_3^+ ions (data of Il'in, Afrosimov and Fedorenko[21]) and electrons (data of Newhall[57]). The designations of the primary particles are given in the figure.

hydrogen by H^+ and H_2^+ the cross section is two orders of magnitude higher (approximately 5×10^{-17} cm^2). These experimental results indicate that there is also a strong interaction in ion-molecular collisions.

A suggestion has been made in reference 21 that the maximum in $\sigma_{H_2^+}(v)$ is due to ordinary one-electron charge exchange, whereas the maximum in the $\sigma_{H^+}(v)$ curve is due to dissociative capture. Beyond the maximum in the cross section for formation of the secondary ions H_2^+ and H^+ the one-electron ionization process becomes important. It has also been established experimentally that most of the fragment protons have energies below 7 ev. The energy of the secondary H_2^+ ions is lower than this.

Il'in et al.[23] investigated the formation of the fragment ions O^+, O^{2+}, N^+ and N^{2+} in the passage of the hydrogen ions H^+ and H_2^+ through air. It is important to note that in this case the yield of atomic fragment ions O^+ and N^+, as compared with the undissociated secondary ions O_2^+ and N_2^+ may reach approximately 50%.

7. Stripping of Primary Ions

Mass spectra frequently exhibit lines that correspond to non-integral mass numbers. This effect, which is due to stripping of the primary ions in the residual gas, was first explained by Mattauch.[58] The first data on the cross section σ_{12}^l for various ions (energies of 10 and 20 kev) were reported in reference 10. For the heavy ions Ba^+, Bi^+ and I^+, this cross section was found to be several times 10^{-17} cm^2 at 20 kev. With a further increase in energy there is stripping with the removal of several electrons;[13,14,59] the stripping cross section increases rapidly. Table IV lists data from reference 14 for the stripping of the A^+ ion with an energy of 75 kev in argon. It is apparent from the table that the cross section falls off as the number of detached electrons increases. The cross section falls off by a factor of 4 or 5 for each successive electron removed.

Korsunskiĭ et al.[59] observed a maximum in σ_{12} in only one case: $N^+ \rightarrow N^{2+}$ at approximately 900 kev. It is probable that in stripping processes in which several electrons are removed the maximum occurs at a higher energy of the primary ions.

The dependence of the stripping cross section on the structure of the target atom is still not well understood. Apparently the ionic stripping cross sections increase with increasing charge of the nucleus in the same way as the cross sections for the formation of multiply-charged ions increase with increasing charge of the nucleus of the primary ion.[13]

TABLE IV.
Cross section for stripping of A^+ ions in argon according to the data of Kaminker and Fedorenko[14]

Transition	σ_{1k}^l(cm^2)
$A^+ \rightarrow A^{2+}$	1.4×10^{-16}
$A^+ \rightarrow A^{3+}$	2.5×10^{-17}
$A^+ \rightarrow A^{4+}$	6.0×10^{-18}
$A^+ \rightarrow A^{5+}$	1.8×10^{-18}

Information on stripping of hydrogen and helium atoms over a wide energy range is given in a recently-published survey by Allison.[68]

If the primary ion is a molecular ion the dissociation of this ion can result in the formation of fragment primary ions. The dissociation of molecular H_2^+ ions in the energy range 100 — 200 kev has been investigated in reference 60; the same effect has been studied between 5 and 180 kev in reference 61. The dissociation of H_3^+ and N_2^+ ions with energies between 5 and 30 kev has been studied in reference 10.

III. SCATTERING IN IONIZATION COLLISIONS

8. General Remarks

The investigation of scattering of atomic particles is of two-fold interest. First, an analysis of the data on the angular distributions allows us to determine the potential energy of the interaction of the particles as a function of the distance $U(r)$ between their nuclei. Secondly, it is possible to obtain information on the conditions for which various inelastic processes can take place; for example, the depth of penetration of the shell and inelastic energy loss.

The analysis of data on elastic scattering of primary ions on gas atoms is based on classical mechanics. Classical ideas can be used because even in the ev energy range the de-Broglie wavelength of the ion is small compared with the dimensions of the atom: quantum-mechanical diffraction effects are important only at very small angles (less than 1°).[62] In the ev region elastic scattering predominates; hence it is relatively simple to set up an experiment and to analyze the data. Many

investigations have been carried out in the ev region with the purpose of determining the form of the function U(r) for various ion-atom pairs. This work has shown that at distances of $2-3 \times 10^{-8}$ cm the attractive polarization forces predominate while at smaller distance the Coulomb repulsive forces due to the nuclei (shielded by electrons) predominate. The results of this work are considered in detail by Massey and Burhop.[3]

Significant scattering of atomic particles with energies in the kev region can result only from repulsive forces, which are much larger than the attractive forces. However, an analysis of the experimental data for the kev region is complicated by the fact that the contribution of inelastic scattering (in particular, scattering with stripping of the primary ions) increases sharply as the deflection angle is decreased. This experimental result was first established in the work of the author[11] and was subsequently verified by other investigators.[14,15,26] Nonetheless, as Firsov has shown,[62] classical ideas can also be used to analyze inelastic scattering of primary ions with energies in the kev region if the inelastic energy loss is small compared with the kinetic energy of particles. In these cases the kinematics of inelastic scattering is the same as the kinematics of elastic scattering.

Starting from this result, Everhart and his colleagues,[24-27] in analyzing the data obtained from scattering of He^+, Ne^+ and A^+ in argon, found that the interaction of atomic particles in the kev energy region can be represented by a shielded Coulomb potential:

$$U(r) = \frac{Z_1 \cdot Z_2 e^2}{r} e^{-r/a}, \qquad (8.1)$$

where Z_1 and Z_2 are the charges of the nuclei in the colliding particles and a is the shielding radius. In this case

$$a = a_0 (Z_1^{2/3} + Z_2^{2/3})^{1/2}, \qquad (8.2)$$

where a_0 is the radius of the first Bohr orbit.

Firsov[63] has made a theoretical calculation of the function U(r) for distances $r < 1 \times 10^{-8}$ cm. According to this calculation

$$U(r) = \frac{Z_1 \cdot Z_2 e^2}{r} \chi\left([Z_1^{1/2} + Z_2^{1/2}]^{2/3} \frac{r}{a}\right), \qquad (8.3)$$

where χ is the Fermi-Thomas shielding function.

All calculations of U(r) are usually carried out for a coordinate system fixed in the center of mass. The determination of the differential cross sections in the center-of-mass system using the data on scattering of the primary particles is simple when $m_1 \leq m_2$ (m_1 is the mass of the primary ion and m_2 is the mass of the atom). When $m_1 > m_2$, there is a limiting scattering angle (ϑ_{max}) in the laboratory system for the particle of mass m_1, and the relation between the deflection angle and the velocity is not unique.[6] In this case, the use of the center-of-mass system becomes highly complicated. In the present paper we consider only cases for which $m_1 \leq m_2$, so that no ambiguity of this kind exists.

The collisions of the primary ions with the gas atoms are characterized by a change in the direction and magnitude of the velocities of both colliding particles. For this reason we actually observe not only scattering of the primary particles, but scattering of the recoil atoms or secondary ions as well. Inelastic scattering of the secondary ions does not give unambiguous results in the laboratory system. The ambiguity, like the ambiguity in scattering of the primary particles, depends on the mass ratio and follows from the conservation of energy and momentum. From the conservation of energy and momentum we can obtain a relation between eight quantities: m_1, m_2, v_0, v_1, v_2, ϑ, φ and E, where v_0 is the initial velocity of the primary particle (or relative velocity if the second particle, the gas atom, can be regarded as immobile before the collision), v_1 and ϑ are the velocity and deflection angles of the primary particle after the collision, v_2 and φ are the velocity and emission angles of the second particle, and E is the inelastic energy loss. Figure 10 shows a velocity diagram for inelastic scattering of particles with the same mass ($m_1 = m_2$).

In an inelastic collision the relative velocity (v_0) is reduced. Hence the deflection of the second particle is characterized by a limiting emission angle

$$\varphi_{max} = \cos^{-1} \sqrt{\frac{(m_1+m_2)}{m_2} \frac{E}{T_0}} \qquad (8.4)$$

(T_0 is the initial kinetic energy of the primary

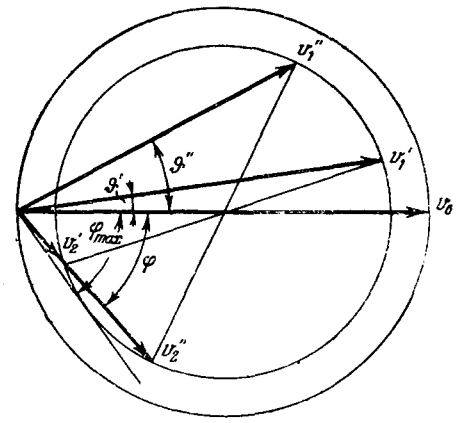

FIG. 10. Velocity diagram for inelastic collisions between two particles with the same mass.

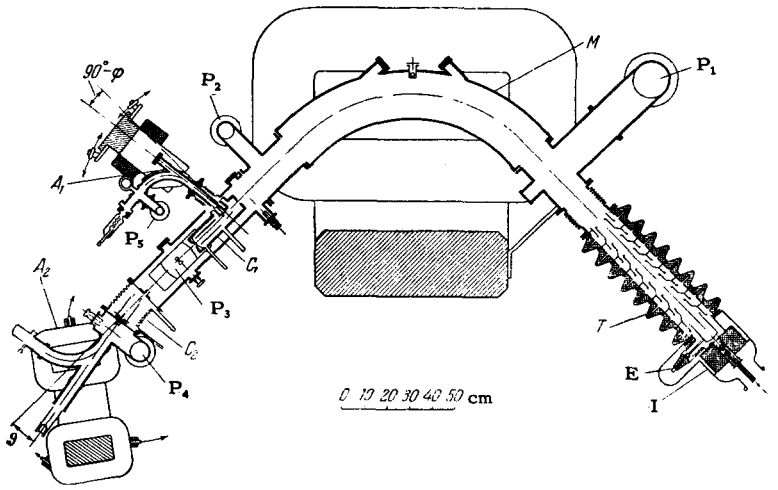

FIG. 11. Schematic diagram of the apparatus used to investigate the scattering of primary and secondary ions by Fedorenko, Afrosimov and Kaminker.[11,14,18,19] [I) ion source, E) extraction electrode, T) accelerating tube, C_1) first collision chamber, A_1) secondary-ion analyzer, C_2) second collision chamber, A_2) primary-ion analyzer, P_1, P_2, P_3, P_4, P_5) pumps.]

particle). It is apparent from Fig. 10 that the limiting emission angle corresponds to only one value of the velocity of the second particle. For all other angles $\varphi < \varphi_{max}$, however, a given value of φ corresponds to two values of the velocity of the second particle, v_2' and v_2'', each of which corresponds to a definite velocity (v_1' and v_1'') and deflection angle (ϑ' and ϑ'') of the primary particle. Below we will use the designation "soft" scattering to denote the case in which the velocity of the second particle is the smaller value (v_2', v_1', ϑ') and "hard" scattering to denote the case in which the velocity is the higher value (v_2'', v_1'', ϑ'').

Thus, one expects the angular distribution of the secondary ions in inelastic collisions to exhibit two energy groups. The difference in energy for these groups should increase with decreasing emission angle φ and should vanish altogether when $\varphi \to \varphi_{max}$. The ambiguity described here, as will be made clear below, facilitates the observation of an angular correlation in inelastic processes when one measures scattering in the laboratory coordinate system.

9. Experimental Investigation of the Angular Distribution

The determination of the absolute differential scattering cross sections per unit solid angle represents a fairly difficult experiment; this measurement requires good angular resolution and a careful analysis of the geometry of the experiment. The geometrical conditions required to study scattering on a gas target were first considered by Jordan and Brode[64] and have been considered in greater detail in references 14 and 65. In elastic scattering of primary particles at small angles, in practice it is essentially impossible to distinguish between the scattered and unscattered particles. In those cases in which they experience a change in e/m (i.e., charge or mass) as a result of an inelastic collision, the primary ions can be distinguished from the primary beam by deflection in a magnetic field. This technique makes it possible to study scattering with a change of e/m at very small angles.[14] In the kev energy region the primary particles are scattered within a few degrees of the initial direction while the secondary ions are more or less scattered at 90° to the primary beam. This situation makes the problem of separating the primary and secondary ions somewhat easier.

The differential scattering cross sections (for primary and secondary atoms) are determined from the general formula

$$\frac{d\sigma}{d\omega_\vartheta} = \frac{i_2(\vartheta)}{i_1}\frac{1}{n}S(\vartheta)\text{cm}^2/\text{steradian} \qquad (9.1)$$

where i_1 is the primary ion current, $i_2(\vartheta)$ is the current due to particles which are scattered at an angle ϑ and extracted by the collimator, n is the density of atoms in the gas target, and $S(\vartheta)$ is a geometric factor that takes account of the change in the effective dimensions of the scattering volume and the solid angle defined by the apertures in the collimator when its axis makes an angle ϑ with the primary beam. All the experimental data on angular distributions for primary and secondary ions in the present paper are given in the laboratory coordinate system.

Figure 11 is a schematic diagram of the apparatus used in most of the work reported here on the scattering of primary and secondary ions. The monochromator (M) provides a primary beam with a known energy distribution and small divergence angle (±0.25°). The first collision chamber and the fixed analyzer which is attached to it are used for investigations of secondary ion scattering.

The collimation of a beam of secondary ions characterized by an emission angle φ with respect to the direction of the primary beam occurs inside the equipotential volume of the collision chamber. Then the secondary ions pass through a system of grids; the energy distribution of the ions in this system is determined by retarding-field techniques. The secondary ions which pass through the grids are then accelerated and charge analyzed in a magnetic analyzer. The ions are detected in an open electron multiplier, the output of which is fed to an electrometer amplifier. The sensitivity of the detection system is 5×10^{-18} amp/div. The construction of this device makes it possible to study values of φ ranging from 77° to 92°. The resolution of the system is $\Delta\varphi \sim \pm 1.25°$. A detailed description of the apparatus used for studying the angular and energy distributions of secondary ions has been given in reference 18.

The second collision chamber and analyzer are used for studies of primary ion scattering and provision is made for analysis of charge states.

The analyzer (A_2) can be rotated about the center of the collision chamber through an angle $\vartheta = \pm 17°$ with respect to the primary beam. The resolving power of the system is $\Delta\vartheta \sim \pm 0.5°$. The ions are detected by a Faraday cage or by an electron multiplier connected to a vacuum-tube electrometer. A detailed description of the primary-ion analyzer has been given in reference 14.

In the work reported here the primary ion current varied between 0.1 and 1.0×10^{-6} amp. The pressure of the gas being studied in the chamber was $1 - 1.5 \times 10^{-4}$ mm Hg. The pressure in the other parts of the apparatus was maintained at better than 5×10^{-6} mm Hg by means of a system of differential pumping.

10. Scattering of Primary Ions with a Change of e/m

The first information concerning scattering of primary ions with a change of e/m (as a result of ion stripping, electron capture by doubly charged primary ions, or dissociation of molecular ions) was reported by us in references 10 and 11. An investigation[15] of the negative-ion scattering accompanied by a change in charge, carried out at 5 — 30 kev, indicated that ionization-exchange processes were intimately related with scattering and that the scattering features were peculiar to each inelastic process. Subsequently a more detailed investigation was carried out by us to study scattering of A^+ ions in the energy range 50 — 150 kev.[14] Everhart and his coworkers[26,27] studied scattering of He^+, Ne^+ and A^+ involving transitions to various charge states; this work was carried out in the same energy region but covered a wider angular range (±40°), with the exception of the region between 0 and ±4°. The results of the works cited above were found to be in agreement with each other.

The curves of Fig. 12 taken from reference 14, show the angular distributions for scattering of A^+ ions in charge states 0, 1, 2, 3, 4 and 5. The fast argon atoms produced as a result of electron capture by the primary A^+ ion beam are scattered with charge 0. Because a "symmetric" pair is involved (A^+–A), the formation of fast argon ions must be attributed primarily to resonance charge exchange. The charge state designated by 1 refers to the scattering of primary A^+ ions which experi-

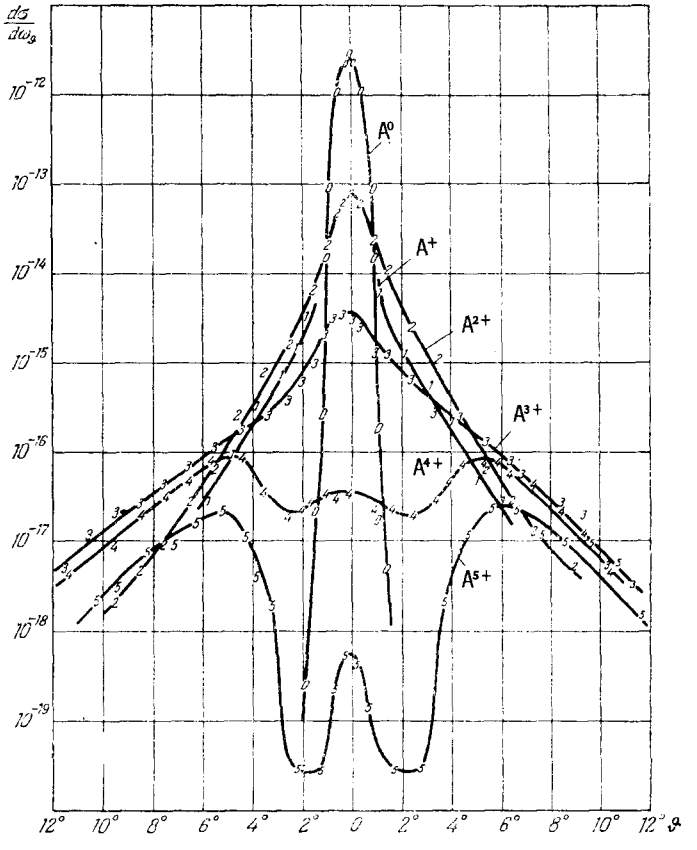

FIG. 12. Scattering of A^+ ions in charge states 0, 1, 2, 3, 4 and 5. The initial energy of the primary ions $T_0 = 75$ kev. The collision chamber is filled with argon at a pressure of approximately 2×10^{-4} mm Hg. The absolute value of the differential scattering cross section (logarithmic scale) is plotted in units of cm^2/steradian and the angle (ϑ) is plotted in degrees along the horizontal axis. The experimental points are denoted by the numbers corresponding to the charge of the primary particle after the collision. [Data of Kaminker and Fedorenko.[14]]

ence elastic collisions (or ionization collisions with gas atoms). The charge states denoted by 2, 3, 4 and 5 refer to the scattered primary ions that experience electron stripping. From an analysis of Fig. 12 one is easily convinced that as the charge increases the angular distribution of the particles becomes more and more "diffuse." It is natural to assume that the inelastic energy losses increase as the charge of the incoming particles increases. Whence it follows that at larger deflection angles of the primary ions there is an increase in the relative probability for processes which require a higher excitation energy. This basic feature of inelastic scattering has been indicated above (Sec. 8).

Another noteworthy feature is the peculiar shape of the angular distribution curves for the most highly ionized states, 4 and 5. These curves exhibit three peaks: a central peak at $\vartheta \to 0°$ and two symmetrically located side peaks. An angular distribution of this type was first reported by us in reference 14 and was called "irregular," in contrast with the "regular" angular distribution, which exhibits a single central peak (as, for example, in scattering for charge 0 or 2).

In order to give some idea of the change in the shape of the angular distribution curves for scattering with stripping as a function of increasing kinetic energy, Fig. 13 shows curves for the transition $A^+ \to A^{4+}$ for three values of the energy of the A^+ ion. It is apparent that as the energy increases all the maxima increase and the side maxima appear at smaller angles. Thus, as the energy increases the angular distribution becomes narrower and more "regular."

It has already been indicated (Sec. 3) that Russek[30] has proposed a phenomenological theory for the interpretation of the data on scattering accompanied by stripping. The theoretical curves

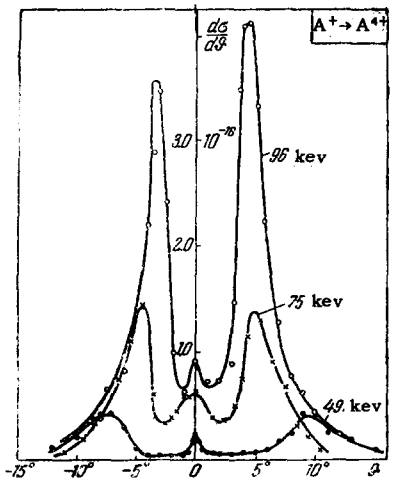

FIG. 13. Modification of the angular distribution for scattering with stripping of the primary ions ($A^+ \to A^{4+}$) as the energy is increased from 49 to 75 and 96 kev. [Data of Kaminker and Fedorenko.[14]]

obtained by Russek exhibit the same general features as the angular distrigution curves obtained by Everhart[27] which are similar to the curves in Figs. 12 and 13.

11. Scattering of Secondary Ions

Up to the present time it has generally been assumed that the secondary ions which are formed in a gas in ion-atom collisions are slow, i.e., it is assumed that the velocities of these ions are essentially thermal. The results of recent work reported by us[18,19] indicate that this assumption does not apply to all secondary ions. Some of the secondary ions, especially multiply-charged ones, have energies of several tens and even hundreds of electron volts. The angle and energy distributions of the secondary ions and the angular distribution of the primary ions are extremely peculiar. In reference 19 an investigation was made of the angular distributions of secondary argon ions (charge ranging from 1 to 5) produced in the ionization of argon by Ne^+ and A^+ ions; the angular distributions of the secondary neon ions (charge ranging from 1 to 3) produced in the ionization of neon by A^+ ions was also studied. The initial energy of the primary ions was varied between 10 and 150 kev. The energy distributions were obtained by studying the angular distributions of the secondary ions measured at different "retardation levels" (the energy setting in the discriminator). This yielded angular distributions of secondary ions with initial energies greater than the retardation level.

The angular distributions for the secondary argon ions with charges 1, 2, 3, 4 and 5 obtained in this work are shown in Fig. 14. The primary beam also contained A^+ ions with an energy of 75 kev. Along the vertical axis is plotted the differential cross section in relative units (I_φ); the emission angle φ is plotted along the horizontal axis. In all cases the value of I_φ at maximum is taken as 100%. It is difficult to make quantitative measurements of the energy distributions of the secondary ions in this work[19] since a considerable fraction of the ions with energies of the order of 1 ev do not reach the detector because there are weak fringing magnetic fields, which cannot be completely eliminated. There is also a distortion in the angular distribution for ions with energies up to 10 ev. This distortion is indicated by the spreading of the angular distribution in the region $\varphi > 90°$. In spite of these effects, an examination of Fig. 14 allows us to distinguish two basic features of the secondary-ion

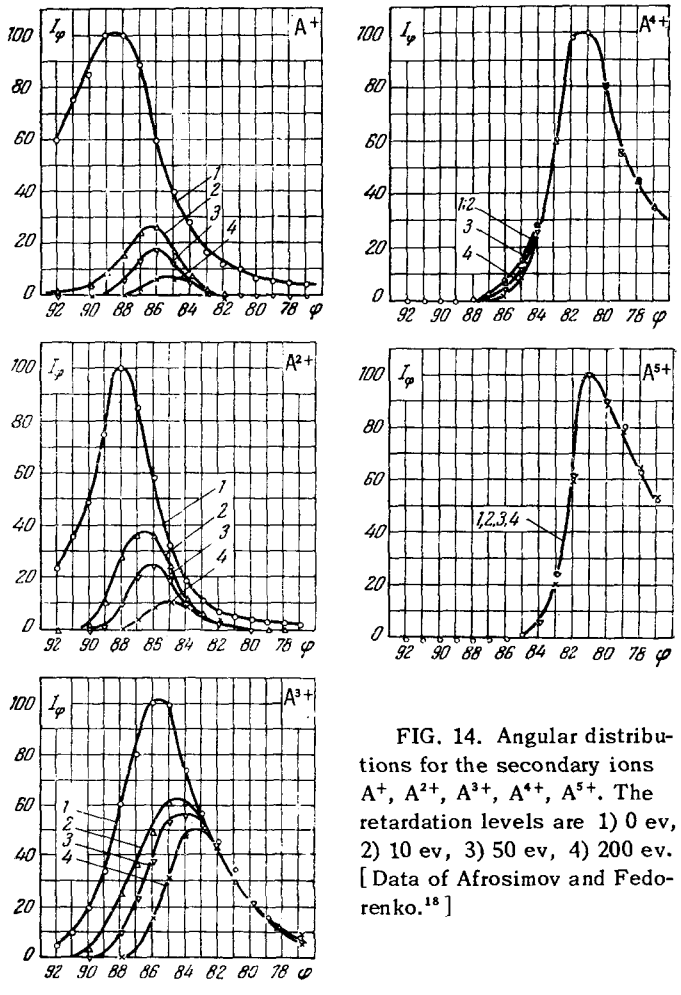

FIG. 14. Angular distributions for the secondary ions A^+, A^{2+}, A^{3+}, A^{4+}, A^{5+}. The retardation levels are 1) 0 ev, 2) 10 ev, 3) 50 ev, 4) 200 ev. [Data of Afrosimov and Fedorenko.[18]]

angular distribution curves. With an increase in the charge of the secondary ion the maxima in the angular distribution curve are shifted towards smaller emission angles (i.e., in the direction of the primary ion beam); at the same time there is an increase in the mean energy of the secondary ions. For example, the angular distributions for the ions with charges 4 and 5 contain for the most part ions with energies greater than 200 ev. An analysis of the experimental data of references 18 and 19 indicates that the slow secondary ions are due primarily to soft scattering while the ions with higher energies arise as a result of hard scattering.

An idea of the change in the secondary-ion angular distribution with increasing primary-ion energy can be obtained from Fig. 15, which shows the angular distributions for the secondary A^{4+} ions measured in reference 19 for two values of the primary-ion energy. It is apparent that with an increase in the energy of the primary ions the maxima in the angular distribution appear at larger emission angles and the number of secondary ions

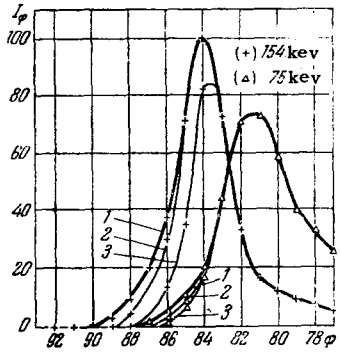

FIG. 15. Angular distribution for secondary A^{4+} ions, measured at the same retardation level for two energies of the primary ion – 75 and 154 kev. The retardation levels are 1) 0, 2) 50, 3) 200 ev. [Data of Afrosimov and Fedorenko.[18]]

with small energies increases, i.e., hard scattering becomes less important.

It has also been shown in reference 19 that for singly charged secondary ions the mean energy falls off as the ratio m_2/m_1 increases.

12. Close Approach of Nuclei and Inelastic Processes

A comparison of scattering of primary and secondary ions yields a qualitative explanation of the peculiar features in the angular distribution curves. We proceed by studying essentially equivalent collision processes for atomic particles that are similar in structure, for example, stripping of the A^+ ion and ionization of the argon atom with the removal of the same number of electrons. A comparison of the corresponding angular distributions for primary and secondary ions obtained in references 14 and 19 reveals certain similarities. The most characteristic similarity is found in processes which require relatively high excitation energies and in which 3, 4, or 5 electrons are detached. In these processes the angular distribution of the secondary ions is dominated by the ions which experience hard scattering. The primary-ion angular distribution is irregular and is characterized by large side peaks. It is apparent that the side peaks also are due to hard scattering. In reference 19 it has been established that for equivalent ionization and stripping processes the experimental values of φ (corresponding to the peak in the secondary-ion angular distribution) and ϑ (corresponding to the side peak in the primary-ion angular distribution) are what one would expect on the basis of conservation of charge and momentum. Similarly, the positions of the minima in the irregular angular distributions are found to be in agreement with the limiting emission angle for the secondary ion (φ_{max}).

In processes of the other kind, which require less energy (for example, one-electron charge exchange), the angular distribution of the second-

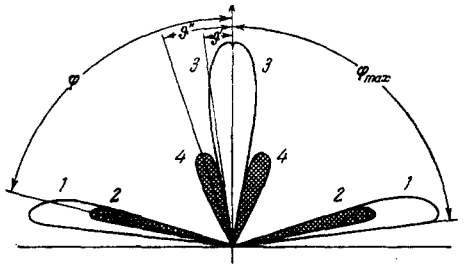

FIG. 16. Graphic representation of the angular distribution of equivalent ionization processes in the shells of colliding atomic particles. The vertical axis denotes the direction of the primary beam. The designations of the angles are the same as Fig. 10. Soft scattering of the secondary ion is shown by Curve 1 and of the primary ion by Curve 3. Hard scattering of the secondary ion is shown by Curve 2 and of the primary ions by Curve 4.

ary ions is dominated by those ions which experience soft scattering; on the other hand, the angular distribution of the fast neutral atoms is regular.

In the general case, an inelastic collision that involves equivalent ionization processes in the shells of both particles can be characterized by a combination of soft and hard scattering. The general case is illustrated by the polar plot of Fig. 16.

According to classical mechanics, if the scattering is due to repulsive forces only an increase in the deflection angle of the primary particles must correspond to a reduction in the impact parameter and the distance to which the nuclei of the colliding particles approach. We conclude therefore that in a given inelastic process hard scattering always corresponds to a closer approach of the nuclei.

In estimating the distance of closest approach (T_0) for small deflection angles ($\vartheta < 15°$) it may be assumed that

$$r_0 \simeq p_0, \tag{12.1}$$

where p_0 is the impact parameter corresponding to deflection through an angle ϑ. A determination of the absolute magnitude of the impact parameter p_0 can be made from the experimental data on the angular distribution of scattered primary particles by means of the relation:

$$p_0^2 = 2\int_{\vartheta_0}^{\pi/2} \frac{d\sigma}{d\omega_\vartheta} \sin\vartheta\, d\vartheta. \tag{12.2}$$

In Eq. (12.2) $\frac{d\sigma}{d\omega_\vartheta}$ is the total differential cross section, obtained by summing the differential scattering cross sections for all charge states with the same deflection angle.

This procedure (based on the considerations given in Sec. 8) has been carried out in references 11, 14 and 26. Under these conditions the total angular distribution

$$\frac{d\sigma}{d\omega_\vartheta} = f(\vartheta), \tag{12.3}$$

obtained by superposing angular distributions of different shapes (regular and irregular), is found to fall off monotonically with increasing values of ϑ, as is to be expected for true elastic scattering.[62]

The estimates of r_0 carried out this way in references 11, 14 and 26 show that all primary-ion stripping processes take place when the distances between the nuclei become smaller than atomic dimensions ($r_0 < 1 \times 10^{-8}$ cm). Processes that require a relatively large energy (for example, stripping with the removal of several electrons) come into play with strong overlapping of the shells (distances of $1 - 5 \times 10^{-9}$ cm).

Atomic ionization processes must take place under the same conditions as those which obtain for stripping of primary ions. This conclusion is supported by the similarities in the angular distributions of the primary and secondary ions described above.

Elastic processes that involve a small inelastic energy loss (for example, one-electron charge exchange) predominate at distances greater than atomic dimensions. Hence, in one-electron charge exchange or in optical excitation the cross section and its velocity dependence are determined basically by the individual features of the energy levels of the outer electrons[3] (cf. Fig. 6).

Ionization processes that occur in overlapping of the shells must undoubtedly involve the excitation of many electrons, as is assumed in the quasi-molecule hypothesis. It is reasonable to expect that in this case the ionization cross section is affected by the more general features of the colliding particles: the nuclear charges, the number of nuclei (in molecular ions), the dimensions of the particles and so on. As indicated above (Secs. 2, 5, 6, and 7), the available experimental data for total ionization cross sections and the cross sections for the formation of multiply charged ions exhibit a general tendency toward increasing cross section with increasing charge of the nuclei of the colliding particles. This result also follows from the analysis given by Firsov.[29]

The change in the shape of the angular distribution curves which occurs as the velocity is increased allows us to ascertain the conditions favorable for stripping and ionization collisions. Using elementary ideas it can be shown that the cross section for ionization processes is proportional to the product of two quantities: the area of

a circle of radius equal to the maximum impact parameter for which the required depth of penetration is possible and the mean probability of the process within the circle. Hence, these processes appear first in central (head-on) collisions because the maximum depth of penetration for a given velocity obtains for a central collision. This result is verified by the fact that at small energies stripping is characterized by a sharply defined irregular angular distribution in which only the side peaks appear. Apparently the effective impact parameter increases when the velocity increases; on the other hand, the probability is larger for smaller values of this parameter. This behavior is indicated by the increase in the side peaks as they appear at smaller and smaller angles, the appearance of the central peak due to soft scattering, and, finally, the fact that the irregular distribution becomes regular (cf. Figs. 13 and 15). Apparently the ionization processes come into play in a regular sequence as the velocity is increased, and following the growth of the inelastic energy losses required for them to occur. Under these conditions the low-energy processes and elastic scattering are no longer features of strong overlapping but are to be associated with a remote interaction.[11]

13. Inelastic Energy Losses

A direct experimental determination of inelastic energy losses has been carried out in reference 18 in collisions of A^+ and Ne^+ ions with argon atoms, which lead to the formation of secondary argon ions with charges ranging from 1 to 6. The initial energy of the primary ions (T_0) was 75 kev. In reference 18 the following expression is given for the relation between the inelastic energy loss (E), the kinetic energy (T_2) and the emission angle (φ) of the secondary ions:

$$E(\varphi) = 2\sqrt{\left(\frac{m_2}{m_1} T_2 \cdot T_0\right)} \cos\varphi - \frac{m_1+m_2}{m_1} T_2. \quad (13.1)$$

It is apparent from Eq. (13.1) that in order to determine $E(\varphi)$ it is sufficient to measure $T_2(\varphi)$ because the remaining quantities (m_1, m_2, T, φ) can be found from the experimental conditions.

The energy of the secondary ions is determined by the retarding-field method. So-called "retardation" curves are taken for ions of a given charge at different emission angles. Figure 17 shows retardation curves obtained for the secondary A^{3+} ions formed in the ionization of argon by Ne^+ ions with an energy of 75 kev. Along the vertical axis is plotted the ratio of the secondary current (i_2)

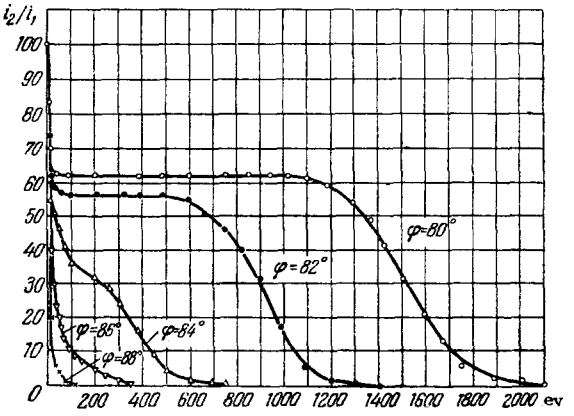

FIG. 17. Typical retardation curves.

which passes through the collimator and retarding grids to the primary current (i_1); the retardation level in electron volts is plotted along the horizontal axis. In order to allow a more graphic comparison of the energy distribution of the secondary ions at different emission angles all curves are drawn from the point at which there is no retardation. It is apparent from Fig. 17 that at large emission angles (86°, 88°) the retarding curve falls off monotonically. As the emission angle is reduced a well defined "step," which separates the hard and soft scattering, is observed. The average kinetic energy of the hard component of the secondary ions at a given emission angle $\overline{T}_2(\varphi)$ is taken as the retardation level corresponding to "half-height" of the step in the corresponding retardation curve. In addition, using Eq. (13.1) it is possible to determine the mean inelastic energy loss $\overline{E}(\varphi)$.

The experimental data of reference 18 indicates that $\overline{E}(\varphi)$ increases as the angle φ is reduced, i.e., as the distance of closest approach becomes smaller.

Firsov[29] has carried out calculations of the inelastic energy loss as a function of the emission angle (φ) for the same ion-atom pairs (A^+–A and Ne^+–A). The theoretical values of $E_t(\varphi)$ obtained by Firsov and the experimental data for $\overline{E}(\varphi)$ from reference 18 (in ev) are given in Table V. It is apparent from an examination of this table that the theoretical values of $E_t(\varphi)$ increase as φ becomes smaller but that this reduction is slower than that of the experimental values. At $\varphi = 78°$ the theoretical and experimental data differ by approximately a factor of 2. However, the agreement may be considered satisfactory because of the approximate nature of the theory. On the other hand, it is also required that the accuracy in the experimental determinations of $\overline{E}(\varphi)$ be increased.

TABLE V. Inelastic energy losses. Theoretical data of Firsov[29] and experimental data of Afrosimov and Fedorenko[18]

	$A^+ - A$				$Ne^+ - A$			
φ	84°	82°	80°	78°	84°	82°	80°	78°
$E_l(\varphi)$	340	400	440	510	350	410	450	510
$\overline{E}(\varphi)$	380	640	890	990	490	560	750	940

It is interesting to note that in reference 18 no significant difference was found in the values of E determined for secondary ions with different charge but for the same emission angle (φ = const). The value of $\overline{E}(\varphi)$ over the entire range of measured emission angles was found to be much greater than twice the ionization energy computed from the ionization potential for the secondary ion with the highest charge (A^{5+}). (In the present case it is assumed that there is simultaneous stripping of the primary A^+ ion, which requires approximately the same ionization energy.) These experimental facts indicate the validity of the statistical considerations developed by Firsov[29] and Russek.[30] Apparently a given distance of closest approach (r_0) corresponds to a definite excitation energy; this energy is always larger than the minimum ionization energy required for the removal of a certain mean number (the most probable) of electrons from the shells of both colliding particles. In this case $\overline{n} = \overline{n}_a + \overline{n}_i$, where $\overline{n}_a$ and $\overline{n}_i$ are respectively the mean numbers of electrons removed from the atom and the ion. There are obviously also collisions in which the values of n, n_a and n_i differ from the most probable values.

It is then natural to ask how the excess excitation energy is dissipated. It has been indicated above (Sec. 3) that the excitation energy is dissipated in auto-ionization, which leads to the formation of multiply-charged primary and secondary ions. It is probable that the excess inelastic energy is partially converted into kinetic energy of the detached electrons; in this case this kinetic energy may be rather large. Blauth has reported[66] that a small fraction of the electrons which arise in ionization of gas atoms by 50-kev protons have energies of several hundred electron volts. In work carried out by Moe and Petsch[34] an investigation was made of the energy spectrum of electrons which are detached in the ionization of neon, argon, and krypton by K^+ ions with energies from 200 to 900 ev. It was found that this spectrum is characterized by several maxima and minima. The positions of the maxima depend on the gas atom and the height depends on the energy of the K^+ ion. The mean energy of the electrons associated with the primary maximum is about 25 ev in neon, about 12 ev in argon, and about 8 ev in krypton. However, it has been pointed out in reference 34 that this angular distribution is characteristic only for an electron emission direction perpendicular to the primary ion beam.

In our opinion, new experimental data on ionization in collisions of ions with atoms will give us a better understanding of the mechanisms involved in the interaction of atomic particles and will thus help to further the development of the theory of atomic collision. Evidence of this trend is found in the theoretical work of Firsov and Russek, who have made use of recent experimental results in formulating new theories.

LITERATURE REFERENCES

I. Books and Review Articles

1. N. Bohr, Penetration of Atomic Particles Through Matter, Danske Vidensk. Selsk. Mat.-fys. Medd. **18**, 8 (1948). (Russ. Transl. IL, Moscow, 1950.)
2. V. L. Granovskiĭ, Электрический ток в газе (Electrical Currents in Gases) Vol. 1, Gostekhizdat, 1952.
3. Massey and Burhop, Electronic and Ionic Collisions, Oxford, 1952. (Russ. Transl. IL, Moscow, 1958.)
4. A. von Engel and M. Steenbeck, Elektrische Gasentladungen, Vols. 1 and 2, Edwards Bros., Ann Arbor, 1944. (Russ. Transl. ONTI, 1935.)
5. L. Loeb, Fundamental Processes of Electrical Discharge in Gases, Wiley, N. Y., 1939. (Russ. Transl. Gostekhizdat, 1950).
6. L. Sena, Столкновения электронов и ионов с атомами газа (Collisions of Electrons and Ions with Gas Atoms) OGIZ, M.-L., 1948.
7. S. K. Allison and S. D. Warshaw, Passage of Heavy Particles through Matter, Revs. Modern Phys. **25**, 779 (1953).

II. Journal References

8. C. W. Sherwin, Phys. Rev. **57**, 814 (1940).
9. J. P. Keene, Phil. Mag. **40**, 369 (1949).
10. N. V. Fedorenko, J. Tech. Phys. (U.S.S.R.) **24**, 769 (1954).
11. N. V. Fedorenko, J. Tech. Phys. (U.S.S.R.) **24**, 784 (1954).
12. N. V. Fedorenko, J. Tech. Phys. (U.S.S.R.) **24**, 2113 (1954).
13. D. M. Kaminker and N. V. Fedorenko, J. Tech. Phys. (U.S.S.R.) **25**, 1843 (1955).
14. D. M. Kaminker and N. V. Fedorenko, J. Tech. Phys. (U.S.S.R.) **25**, 2239 (1955).
15. V. M. Dukel'skiĭ and N. V. Fedorenko, J. Tech. Phys. (U.S.S.R.) **25**, 2193 (1955).
16. Fedorenko, Afrosimov, and Kaminker, J. Tech. Phys. (U.S.S.R.) **26**, 1929 (1956), Soviet Phys.–Tech. Phys. **1**, 1861 (1957).
17. N. V. Fedorenko and V. V. Afrosimov, J. Tech. Phys. (U.S.S.R.) **26**, 1941 (1956), Soviet Phys.–Tech. Phys. **1**, 1872 (1957).
18. V. V. Afrosimov and N. V. Fedorenko, J. Tech. Phys. (U.S.S.R.) **27**, 2557 (1957), Soviet Phys.–Tech. Phys. **2**, 2378 (1958).
19. V. V. Afrosimov and N. V. Fedorenko, J. Tech. Phys. (U.S.S.R.) **27**, 2573 (1957), Soviet Phys.–Tech. Phys. **2**, 2391 (1958).
20. N. V. Fedorenko, Proceedings of the 3rd International Conference on Ionization Phenomena in Gases, Venice, 1957.
21. Afrosimov, Il'in, and Fedorenko, J. Exptl. Theoret. Phys. (U.S.S.R.) **34**, 1938 (1958), Soviet Phys. JETP **7**, 968 (1958).
22. Afrosimov, Il'in, and Fedorenko, J. Tech. Phys. (U.S.S.R.) **28**, 2266 (1958), Soviet Phys.–Tech. Phys. **3**, 2080 (1959).
23. Il'in, Afrosimov, and Fedorenko, J. Exptl. Theoret. Phys. (U.S.S.R.) **36**, 41 (1959), Soviet Phys. JETP **9**, 29 (1959).
24. Everhart, Carbone, and Stone, Phys. Rev. **98**, 1045 (1955).
25. Everhart, Stone, and Carbone, Phys. Rev. **99**, 1287 (1955).
26. Carbone, Fuls, and Everhart, Phys. Rev. **102**, 1524 (1956).
27. Fuls, Jones, Ziemba, and Everhart, Phys. Rev. **107**, 704 (1957).
28. H. B. Gilbody and J. B. Hasted, Proc. Roy. Soc. (London) **A240**, 382 (1957).
29. O. B. Firsov, J. Exptl. Theoret. Phys. (U.S.S.R.) (in press).
30. A. Russek and M. Tom Thomas, Phys. Rev. **109**, 2015 (1958).
31. Fogel', Krupnik, and Safronov, J. Exptl. Theoret. Phys. (U.S.S.R.) **28**, 589 (1955), Soviet Phys. JETP **1**, 415 (1955).
32. De Heer, Huizenga, and Kistemaker, Physica **23**, 181 (1957).
33. D. E. Moe, Phys. Rev. **104**, 694 (1956).
34. D. E. Moe and O. H. Petsch, Phys. Rev. **110**, 1358 (1958).
35. O. Beek and J. Mouzon, Ann. phys. **11**, 737, 858 (1931).
36. J. C. Mouzon, Phys. Rev. **41**, 605 (1932).
37. C. A. Frische, Phys. Rev. **43**, 160 (1933).
38. P. T. Smith, Phys. Rev. **36**, 1293 (1930).
39. J. T. Tate and P. T. Smith, Phys. Rev. **39**, 270 (1932).
40. D. R. Bates and G. W. Griffing, Proc. Phys. Soc. (London) **A68**, 90 (1955).
41. Boyd, Moiseiwitsch, and Stewart, Proc. Phys. Soc. (London) **A70**, 110 (1957).
42. J. B. Hasted, Proc. Roy. Soc. (London) **A205**, 421 (1951).
43. J. B. Hasted, Proc. Roy. Soc. (London) **A212**, 235 (1952).
44. J. B. H. Stedeford and J. B. Hasted, Proc. Roy. Soc. (London) **A227**, 466 (1955).
45. H. B. Gilbody and J. B. Hasted, Proc. Roy. Soc. (London) **A238**, 334 (1957).
46. H. B. Gilbody and J. B. Hasted, Proc. Phys. Soc. (London) **A72**, 293 (1958).
47. A. Jablonski, Z. Physik, **70**, 723 (1931).
48. W. Weizel, Z. Physik **76**, 258 (1932).
49. V. S. Nikolaev, J. Exptl. Theoret. Phys. (U.S.S.R.) **33**, 534 (1957), Soviet Phys. JETP **6**, 417 (1958).
50. Nikolaev, Fateeva, Dmitriev, and Teplova, J. Exptl. Theoret. Phys. (U.S.S.R.) **33**, 306 (1957), Soviet Phys. JETP **6**, 239 (1958).
51. E. Lindholm, Proc. Phys. Soc. (London), **A66**, 1068 (1953).
52. E. Lindholm, Z. Naturforsch. **9a**, 535 (1954).
53. E. Ruchard, Handbuch d. Physik B XXII/2, 75 (1933).
54. W. Bleakney, Phys. Rev. **36**, 1303 (1930).
55. Dukel'skiĭ, Afrosimov, and Fedorenko, J. Exptl. Theoret. Phys. (U.S.S.R.) **30**, 792 (1956), Soviet Phys. JETP **3**, 764 (1956).
56. Ya. M. Fogel' and R. V. Mitin, J. Exptl. Theoret. Phys. (U.S.S.R.) **30**, 450 (1956), Soviet Phys. JETP **3**, 334 (1956).
57. H. F. Newhall, Phys. Rev. **62**, 11 (1942).
58. J. Mattauch and H. Lichtblau, Physik Z. **40**, 16 (1939).
59. Korsunskiĭ, Pivovar, Markus, and Leviant, Dokl. Akad. Nauk SSSR **103**, 399 (1955).
60. K. K. Damodaran, Proc. Roy. Soc. (London) **A239**, 382 (1957).

61. Fedorenko, Afrosimov, Il'in, and Kaminker, J. Exptl. Theoret. Phys. (U.S.S.R.) **36**, 385 (1959), Soviet Phys. JETP **9**, 267 (1959).
62. O. B. Firsov, J. Exptl. Theoret. Phys. (U.S.S.R.) **34**, 447 (1958), Soviet Phys. JETP **7**, 308 (1958).
63. O. B. Firsov, J. Exptl. Theoret. Phys. (U.S.S.R.) **33**, 696 (1957), Soviet Phys. JETP **6**, 534 (1958).
64. E. B. Jordan and R. B. Brode, Phys. Rev. **43**, 112 (1933).
65. I. P. Skal'skaya, J. Exptl. Theoret. Phys. (U.S.S.R.) **24**, 1912 (1954).
66. E. Blauth, Z. Physik **147**, 228 (1957).
67. E. E. Salpeter, Proc. Phys. Soc. (London) **A63**, 1295 (1950).
68. S. K. Allison, Revs. Modern Phys. **30**, 1137 (1958).

Translated by H. Lashinsky